'Fingerprint' Fine Structure in the Solar Decametric Radio Spectrum Solar Physics

E. Y. Zlotnik, V. V. Zaitsev, V. N. Melnik, A. A. Konovalenko & V. V. Dorovskyy

Solar Physics
A Journal for Solar and Solar-Stellar Research and the Study of Solar Terrestrial Physics

ISSN 0038-0938

Sol Phys
DOI 10.1007/s11207-015-0724-x

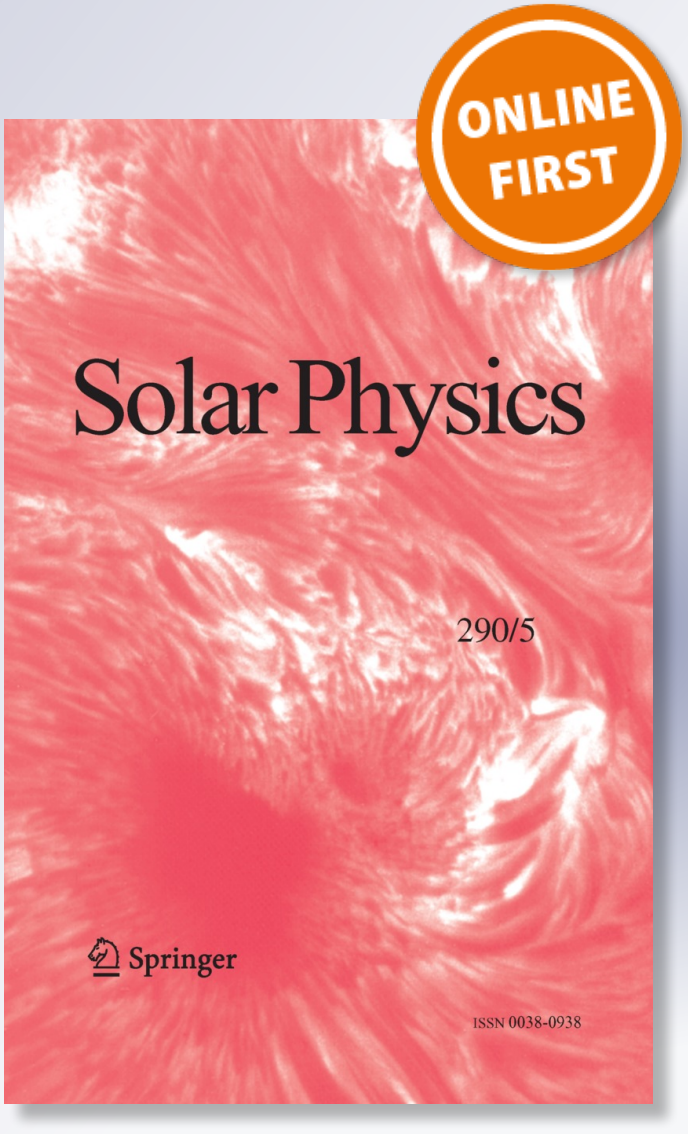

Springer

Solar Phys
DOI 10.1007/s11207-015-0724-x

'Fingerprint' Fine Structure in the Solar Decametric Radio Spectrum *Solar Physics*

E.Y. Zlotnik[1] · V.V. Zaitsev[1] · V.N. Melnik[2] · A.A. Konovalenko[2] · V.V. Dorovskyy[2]

Received: 2 December 2014 / Accepted: 10 June 2015

Abstract We study a unique fine structure in the dynamic spectrum of the solar radio emission discovered by the UTR-2 radio telescope (Kharkiv, Ukraine) in the frequency band of 20 – 30 MHz. The structure was observed against the background of a broadband type IV radio burst and consisted of parallel drifting narrow bands of enhanced emission and absorption on the background emission. The observed structure differs from the widely known zebra pattern at meter and decimeter wavelengths by the opposite directions of the frequency drift within a single stripe at a given time. We show that the observed properties can be understood in the framework of the radiation mechanism by virtue of the double plasma resonance effect in a nonuniform coronal magnetic trap. We propose a source model providing the observed frequency drift of the stripes.

Keywords Radio bursts, type IV · Radio emission, theory

1. Introduction

Decametric sporadic solar radio emission is known to have a great variety of spectral details (Melnik *et al.*, 2005, 2011). It distinctly shows all five main types of the bursts accompanying fast electrons or shock waves propagating through the solar corona, as well as the bursts induced by energetic electrons trapped in the coronal magnetic fields. The radio telescope UTR-2 in Kharkiv, Ukraine (Braude *et al.*, 1978), has been used for more than 40 years for

✉ E.Y. Zlotnik
zlot@appl.sci-nnov.ru

V.V. Zaitsev
za130@appl.sci-nnov.ru

V.N. Melnik
valentin_melnik@yahoo.com

1 Institute of Applied Physics, Russian Academy of Science, 46 Uljanov st., Nizhny Novgorod, Russia

2 Institute of Radio Astronomy, National Academy of Sciences of Ukraine, 4 Chervonopraporna St., 61002 Kharkov, Ukraine

Published online: 30 June 2015

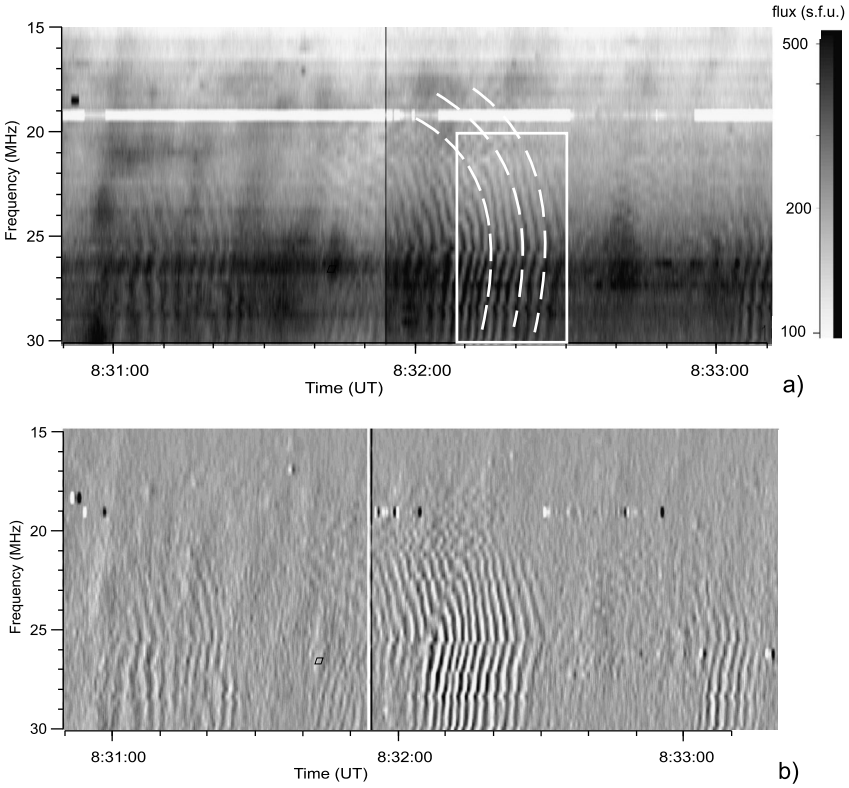

Figure 1 Dynamic spectrum of the solar burst 'fingerprint' on 22 July 2004 (a) and its differential dynamic spectrum (b). The rectangle indicates the portion that is used for the numerical analysis. The dashed lines schematically show the form of the fine structure lines.

observations at frequencies of 10 – 30 MHz. The application of a new back-end with enhanced sensitivity, extended frequency range, and increased frequency resolution resulted in the detection of fine frequency details, the analysis of which enables obtaining information about the physical conditions and processes in the upper corona.

We here study a fine structure in the dynamic spectrum observed on 22 July 2004 against the background of the type IV continuum within the frequencies of 20 – 30 MHz for one and a half minute (Melnik *et al.*, 2008). In 2004, the solar radio emission was observed by only three sections of the UTR-2 radio telescope with an effective area of 30 000 m^2 and an antenna pattern size of $1^\circ \times 13^\circ$. The signal was recorded by a 60-channel spectrometer with a frequency band of 3 kHz for each channel. The frequency spacing between the channels was 340 kHz, which means that the entire working frequency band from 10 to 30 MHz was covered. The location of the channels was chosen so as to eliminate interference. A linear interpolation was applied to fill the gaps between the channels. This 60-channel spectrometer provided a time resolution of 25 ms and a sensitivity of 10^{-23} W m^{-2} Hz^{-1}.

The dynamic spectrum of the burst shown in Figure 1 looks like a fingerprint, and following (Melnik *et al.*, 2008), this term is used for further analysis. The fine structure as a system of quasi-harmonic parallel stripes drifting in time, or the so-called zebra pattern (ZP), is often observed in solar dynamic spectra at meter and decimeter wavelengths (see, for example, Aurass *et al.* (2003) and Chen *et al.* (2011), and reviews by Chernov (2006)

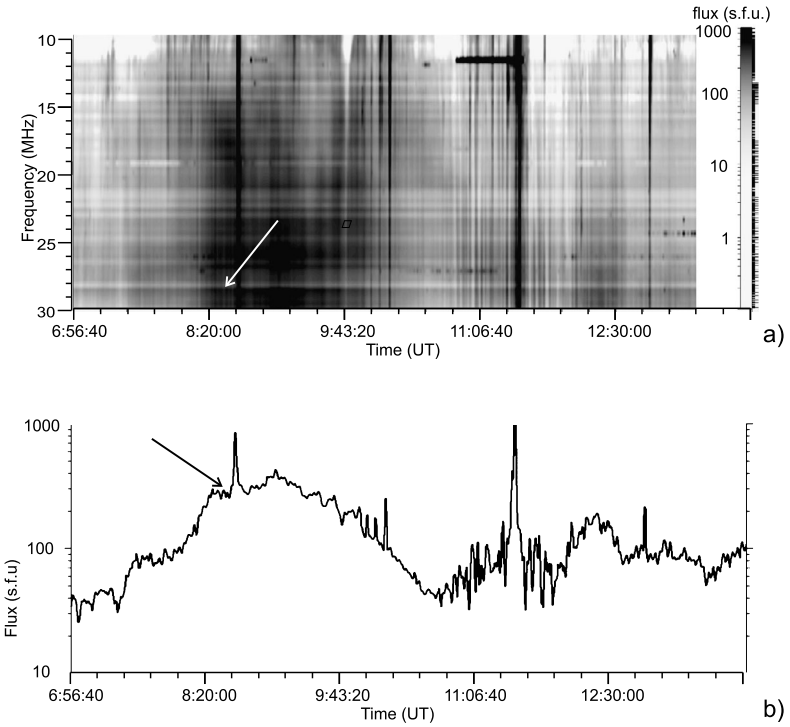

Figure 2 Dynamic spectrum of the type IV burst on 22 July 2004 (a) and its time profile at 30 MHz (b). The time corresponding to the discussed ZP is marked with arrows.

and Zlotnik (2009)). However, at first glance, the burst we study here can hardly be attributed to ZP. Instead, it does not show stripes of enhanced radiation equally spaced in frequency, but quasi-periodic bursts of enhanced radiation; namely fine structure in time, not in frequency domains. Thus, it cannot be considered as a typical ZP and be explained by the double plasma resonance (DPR) effect in a coronal trap. Nonetheless, as shown below, 'the fingerprint' is easily explained in the framework based on the DPR effect, and it really represents some type of usual ZPs.

2. Type IV Burst and Associated Events

To assess the physical context in which this fine structure was observed, we describe the type IV burst against which the fine structure was observed and the associated events. On 22 July 2004 the observations of solar radio emission with the UTR-2 radio telescope were carried out from 08:00 till 12:40 UT. The dynamic spectrum and the time profile (at a frequency of 30 MHz) for the whole session are shown in Figure 2. The enhanced radio emission observed between 08:40 and 10:15 UT is a part of the type IV burst, which seemingly started before 08:00 UT and lasted after 12:40 UT. According to the *Nançay Decametric Array* data,[1] this burst continued at least until 16:00 UT.

[1] http://www.obs-nancay.fr/-Le-reseau-decametrique-.html.

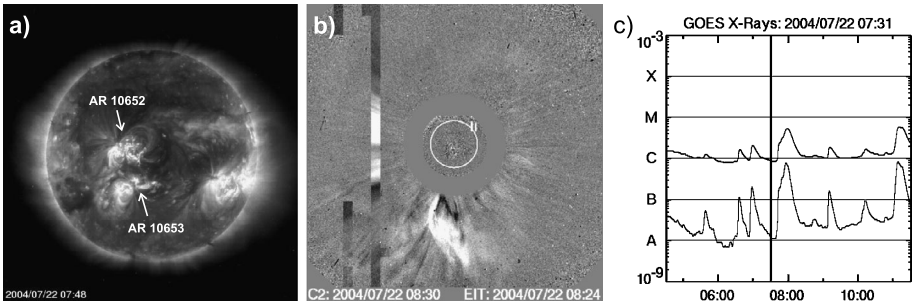

Figure 3 Active regions in UV light observed by SOHO/EIT 191 (a), CME observed by SOHO/LASCO C2 (b), and X-ray flares observed by GOES (c).

In the observed period of time, this burst had a main peak with a flux of 1×10^3 s.f.u. (solar flux unit; 1 s.f.u. $= 10^{-22}$ W m^{-2} Hz^{-1} $= 10^4$ Jy) and two weaker peaks with fluxes of 2×10^2 s.f.u. As usual, the burst consisted of fine structure in the form of fiber bursts and zebra stripes. One of the peculiar properties is that the zebra stripes were observed in groups containing from 5 up to 38 separate stripes in each. About 20 groups were observed between 08:00 UT and 12:30 UT. Further details about this burst can be found in Melnik *et al.* (2008).

Unlike the meter and decimeter zebra structure that is mainly periodical in frequency, the decameter zebra structure is periodical in time. The drift rates of these zebra stripes may have either negative or positive signs. Some stripes may have drift rates of both signs simultaneously. The most remarkable case of a decameter zebra structure is shown in Figure 1. The group of zebra stripes resembling a fingerprint in the dynamic spectrum is the subject of our analysis here.

Nearly simultaneously with the onset of the type IV burst, a partial halo CME was observed by SOHO/LASCO coronagraphs (Figure 3b). The CME moved with a velocity of about 900 km s^{-1} presumably toward the Earth.[2] It was most likely associated with the processes in active region NOAA 10 652 (Figure 3a), in particular, with flares at 07:00 and 08:00 UT, recorded by the GOES spacecraft in X-rays (see Figure 3c). The CME that moved through the coronal plasma and interacted with the high coronal loops that connect active regions NOAA 10 652 and 10 653 appeared to be the source of the type IV burst.

The data of available optical measurements did not give definite information about the formation of the loop or trap configurations, which are necessary to form the non-equilibrium velocity distribution of electrons perpendicular to the magnetic field. However, it is quite possible that such loops existed in the upper corona and that in one of such loop conditions were realized that are suitable for the DPR instability. The mere presence of the ZP on the decameter dynamic spectrum unambiguously testifies the presence of the trap configuration in the source of the observed burst.

3. DPR Effect in the Solar Corona

We briefly recall the DPR effect in the corona (Zheleznyakov and Zlotnik, 1975a, 1975b; Kuijpers, 1975; Winglee and Dulk, 1986; Zheleznyakov, 2000; Kuznetsov and Tsap, 2007; Zlotnik, 2009; Zlotnik and Sher, 2009). It is assumed that a magnetic flux tube is filled

[2] http://cdaw.gsfc.nasa.gov/CME_list/UNIVERSAL/2004_07/univ2004_07.html.

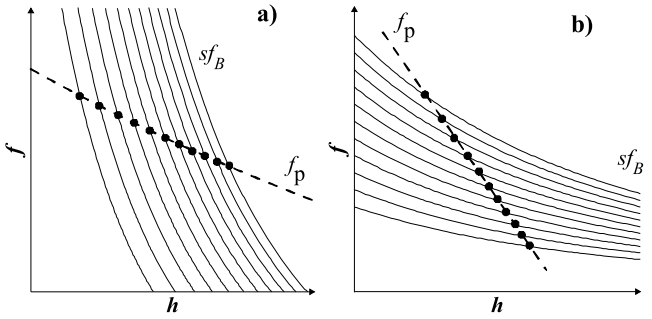

Figure 4 Model of a typical ZP source in the meter-decimeter wave band with different height variations in the electron number density and magnetic field strength. Two panels refer to the cases where the magnetic field changes with the height faster (a) and slower (b) than the electron number density.

with a weakly anisotropic plasma in equilibrium, with electron number density N as well as a small amount of the electrons with electron number density N_e, which have a non-equilibrium velocity distribution perpendicular to the magnetic field:

$$N_e \ll N. \tag{1}$$

Then at the discrete levels where the frequency of the upper hybrid resonance $f_{UH} = (f_p^2 + f_B^2)^{1/2} \approx f_p$ (the last approximate equality is valid under the condition of weak anisotropy $f_B \ll f_p$) coincides with harmonics of the electron cyclotron frequency f_B, *i.e.*

$$f_p = sf_B, \tag{2}$$

enhanced generation of the plasma waves propagating perpendicular to the magnetic field takes place. In these relations, $f_p = (e^2 N/\pi m)^{1/2}$ is the plasma frequency, $f_B = eB/2\pi mc$ is the electron cyclotron frequency, B is the magnetic field, e and m are the electron charge and mass, c is the light velocity, and s is the harmonic number.

Figure 4 shows the model of the ZP source illustrating the DPR effect with different height variations in the electron number density and magnetic field strength along the flux tube at a given time. For simplicity, here we assume that the nonuniform source is elongated vertically in the corona, so that the coordinate along the source is the height h above the photosphere. Evidently, the DPR effect is realized only by different gradients of the magnetic field and electron number density. Radiation stripes arise at the levels corresponding to the intersection points of these curves. The frequency spacing between stripes is determined by the electron cyclotron frequency and the ratio between the gradients of the magnetic field and the electron number density, in other words, by the ratio of typical sizes of the inhomogeneity length scale of the electron number density $L_N = |f_p(\mathrm{d}f_p/\mathrm{d}h)^{-1}|$ and the magnetic field $L_B = |f_B(\mathrm{d}f_B/\mathrm{d}h)^{-1}|$. If the magnetic field changes with height faster than the electron number density, that is, $L_N \gg L_B$, then the frequency spacing is smaller than the cyclotron frequency, which matches the majority of observed ZP events. In the case of the opposite inequality $L_N \ll L_B$, the frequency spacing can be comparable with or exceed the cyclotron frequency. It is important that the DPR regions themselves are very narrow, so that the frequency band of the radiating stripes is narrower than the frequency spacing. This guarantees the appearances of resolved stripes of enhanced intensity in the dynamic spectrum (Zheleznyakov and Zlotnik, 1975a, 1975b).

In addition, the DPR instability has a rather low threshold over the nonthermal electron number density, which is necessary to overcome plasma wave damping due to collisions.

This explains the very frequent appearance of the ZP in the dynamic spectra. An essential part of the plasma mechanism responsible for the creation of solar radio bursts is the nonlinear transformation of the plasma waves that are incapable of escaping from the corona into electromagnetic radiation that easily leaves the source (Zheleznyakov, 2000). There is reason to believe (Zlotnik, Zaitsev, and Altyntsev, 2014) that the process of induced scattering by ions or low-frequency oscillations is preferable for the ZP interpretation than the coalescence of two plasma waves. In the former case, the transformation of plasma waves occurs without significant frequency change; as a result, the striped shape of the spectrum will persist.

Special attention should be paid to the frequency drift of zebra stripes. Evidently, the change of the zebra stripe frequency is determined by the relative change in the magnetic field and electron number density, and it will significantly depend on the ratio of typical sizes of the inhomogeneity of the electron number density L_N and the magnetic field L_B (Figure 4). If in the source where $L_N > L_B$ (Figure 4a) the electron number density remains constant, but the magnetic field decreases with time (this is quite natural for the post-flare stage), then the system of curves in Figure 4a that describes the harmonics of the cyclotron frequency will decrease and the intersection points between the cyclotron harmonics and plasma frequency will move toward higher frequencies. Since these intersection points are the frequencies of the zebra stripes, the decrease in the magnetic field results in the positive frequency drift, that is, the frequencies of the zebra pattern increase when the magnetic field decreases in the source with $L_N > L_B$. In contrast, in the source with faster change in the electron number density over height, when $L_N < L_B$ (Figure 4b), the frequency drift is negative if the magnetic field decreases with time. The ZP frequencies can also change if the magnetic field remains constant, but the electron number density increases or decreases (if the dashed lines move up and down in Figure 4). Independent of the ratio L_N and L_B, the frequency drift is positive if the electron number density increases with time, and negative otherwise.

This model of the ZP source successfully explains the majority of the observed ZP in the meter and decimeter wave band. Specifically, it can explain the many stripes, the dependence of frequency spacing between the stripes on the frequency, the frequency drift, the relatively frequent appearance of ZP in the solar radio emission, the high polarization of radiation in zebra stripes corresponding to the ordinary mode, and the occasional oscillations of the frequency drift velocity (see, for example, Zlotnik, 2009; Winglee and Dulk, 1986; Chen *et al.*, 2011; Zlotnik *et al.*, 2003, and Kuznetsov and Tsap, 2007). The crucial argument in favor of the ZP theory based on the DPR effect was given by Chen *et al.* (2011), who proved that different zebra stripes emerge in spatially separated sources.

4. Interpretation of the 'Fingerprint' Fine Structure

As mentioned above, the 'fingerprint' fine structure we discuss here does not look like a typical ZP slowly drifting in time and consisting of a great number (sometimes several tens) of stripes of enhanced intensity at a given time.

Nonetheless, we assume that the bright stripes in Figure 1 emerged in the DPR regions that corresponded to separate harmonics of the cyclotron frequency. These harmonics have the form of almost vertical arcs, shown by the dashed lines in Figure 1. Here in the part of the event at about 08:32:00 UT, when the frequencies of the zebra stripes reached their minima, the spectrum resembled the usual ZP; the stripes had a mild positive frequency drift. However, the zebra stripe frequencies eventually began to increase sharply (fast positive

drift appeared, and its velocity grew with time), and simultaneously there appeared a low-frequency branch of the stripe with negative frequency drift, where the velocity also grew with time. At first glance, these two branches were not related to each other, but later they joined at a point with an infinitely large frequency drift. This means that they cannot be independent.

Thus, an essential feature of the dynamic spectrum shown in Figure 1 is the fast frequency drift of the zebra stripes and the reversal of the frequency drift within the same harmonic. At each harmonic, there were two frequencies of enhanced radiation at a given time. We consider in detail the portion of the spectrum indicated by a rectangle in Figure 1, where the striped character is seen most clearly. Here the enhanced radiation appeared first at frequencies well separated from each other, then these frequencies become closer, and they merge and disappear at the point with infinite frequency drift. The model of the source should explain the different signs of the frequency drift; at low frequencies it was positive, but then it changed to negative through an infinite drift velocity. In addition, at a given time, no more than two harmonics were observed. It is rather difficult to explain this behavior of the zebra stripes in the framework of the models shown in Figure 4.

4.1. Qualitative Interpretation

We assume, however, that the electron number density changes with height in such a way that its gradient changes in a wide range from rather large values in the upper layers to smaller values in the lower layers. The assumed variations of the plasma frequency with height (coinciding with the electron number density in the source) are given in Figure 5 (dashed lines). We constructed the model of the source in a way similar to that in Figure 4.

We assumed that at some time the radiating harmonics (with harmonic numbers $s-1$, s, and $s+1$) intersect the plasma frequency distribution only in the lower frequency part (Figure 5a). Then three points will appear in the corresponding dynamic spectrum (Figure 5d). When the magnetic field decreases with time, that is, three lines displaying harmonics move down in Figure 5a, the DPR points will shift to higher frequencies and the usual ZP spectrum is formed with the weak positive frequency drift (as follows from Figure 5a, here $L_N > L_B$). When the magnetic field proceeds to decrease and the DPR points shift to even higher frequencies, the gradient of the electron number density increases, and so does the velocity of the frequency drift (Figure 5d). The most important attribute of the model is that with further decrease in the magnetic field, the harmonics start to intersect the line $f_{\mathrm{p}}(h)$ at two points; see in this context the moment t_2 (Figure 5b).

Thus, there are always two points determining the zebra stripe within the same harmonic. In addition, in the high-frequency part of the zebra stripe the ratio of the gradients is opposite to that in the low-frequency part, that is, $L_N < L_B$. This means that the DPR frequencies decrease with the further decrease in the magnetic field, which provides the negative frequency drift. Therefore, in the dynamic spectrum the two branches of the harmonics will approach each other (Figure 5e). Evidently, with further decrease in the magnetic field (Figure 5c, moment t_3), the frequency separation between the DPR points decreases, the DPR points approach each other, and then the harmonic leaves the intersection region with the line $f_{\mathrm{p}}(h)$, *i.e.* the harmonic curve does not have DPR points and disappears from the dynamic spectrum (Figure 5f).

At the moment of touching the curves $f_{\mathrm{p}}(h)$ and $sf_B(h)$, the velocity of the frequency drift is infinite. It is just the behavior of the zebra stripes in the observed spectrum in the selected portion of the fingerprint burst. The apparent almost vertical drift of the zebra stripes is due to the very similar values of the gradients of the magnetic field and electron number density.

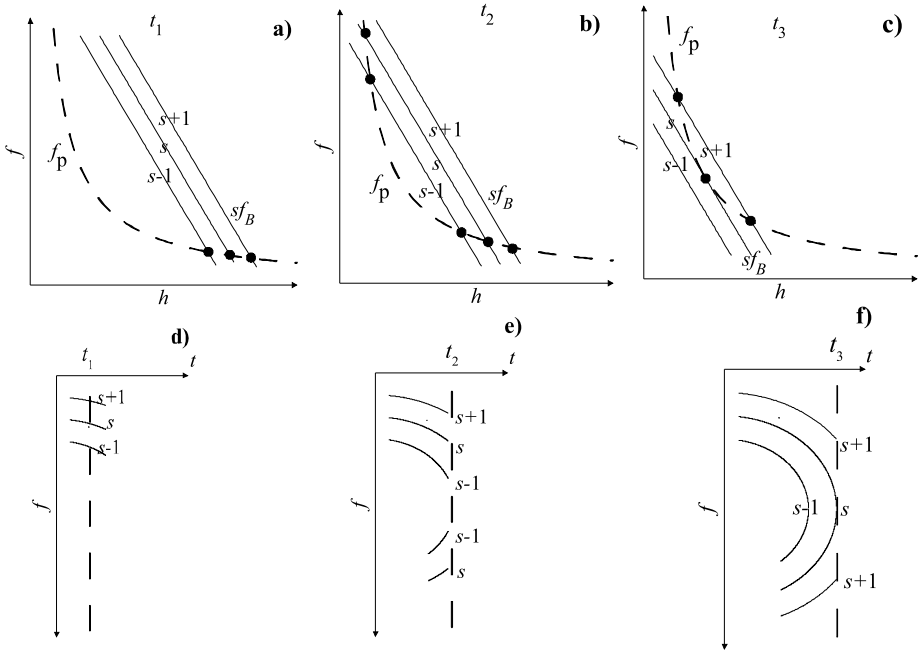

Figure 5 Qualitative interpretation of the fingerprint structure as a set of quasi-vertical arcs. The top panel is the source model at three times $t_1 < t_2 < t_3$; the electron number density remains constant, and the magnetic field decreases in time. The filled circles denote the DPR levels. The lower panel gives the dynamic spectrum with the zebra stripes corresponding to the times t_1, t_2, and t_3.

Thus, the quasi-vertical arc-like ZP structure in the fingerprint event can be explained by the gradual decrease in the magnetic field in the source with electrons that are not in equilibrium in the transverse velocities (perpendicular to the magnetic field), under the condition that the harmonic with a given number has two DPR points at different heights. Herewith, the numbers of harmonics increase from the 'inner' to the 'outer' arcs.

It follows from this argument that the decrease of the magnetic field in time results in the appearance of 'descending' quasi-vertical arcs in the dynamic spectra. It is easy to see that if the magnetic field has increased in time, the harmonics would have moved upward, and the event would have developed according to Figure 5 in the direction from (c) to (a) and from (f) to (d). In this case, the ascending arcs (with the opposite convexity) would have been present in the dynamic spectrum.

The scheme given in Figure 5 qualitatively illustrates the idea with which we explain the observed details of the fine structure in the form of quasi-vertical arcs based on the DPR effect. However, to explain the fingerprint burst shown in Figure 1 and to ensure that such a scheme can be realized under coronal conditions, it is necessary to propose a source model that can provide the observed numerical values of the zebra stripe frequencies and the velocities of the frequency drift under realistic conditions of the solar corona.

4.2. Realistic Model of the Fingerprint Burst Source

Figure 6 shows the enlarged numerical record of the dynamic spectrum shown by a rectangle in Figure 1, where the structure with the resolved stripes is seen most clearly. The lines

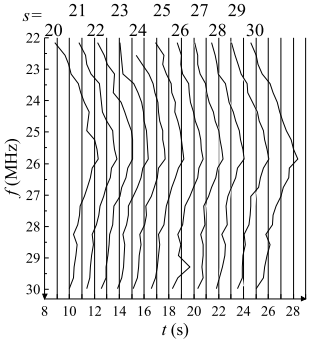

Figure 6 Plots of the dynamic spectrum in the rectangle in Figure 1. The numbers above the graph indicate the numbers of the harmonic numbers of the electron cyclotron frequency used in the proposed source model.

correspond to the peak intensities observed in the zebra stripes. Our purpose is to find the magnetic field and the electron number density variations with height and time that provide the location of the DPR levels at the frequencies corresponding to the observed frequencies of the zebra stripes at each time moment, as well as the successive appearance of the 11 observed harmonics with time. We carried out computations with a time resolution of 1 s. The rectangle in Figure 1a covers the time interval 08:32:09 UT – 08:32:28 UT. We designate below the time in seconds from 08:32:00; for example, the time 08:32:13 UT is denoted $t = 13$.

For simplicity we considered the magnetic flux tube containing non-equilibrium electrons, *i.e.* the ZP source, to be located vertically in the corona, that is, the source distribution is a function of height. As a model for the distribution of the electron number density over height in the decameter radiation sources, we adopted the Newkirk model (Newkirk, 1961):

$$N = 4.2 \times 10^4 \times 10^{4.32 R_S/R}, \tag{3}$$

where $R_S = 7 \times 10^{10}$ cm is the solar radius, R is the distance from the solar center, and N is expressed in cm^{-3}. According to Equation (3), the plasma with electron number density 6×10^6 cm^{-3} $< N < 1.1 \times 10^7$ cm^{-3}, corresponding to the observed frequency band of 22 MHz $< f \approx f_p <$ 30 MHz, is located at heights 5.4×10^{10} cm $< h < 7.0 \times 10^{10}$ cm. Correspondingly, the plasma frequency changes with the height as

$$f_p = 1.84 \times 10^{2.16/(1+h/7)}, \tag{4}$$

where the height h and the plasma frequency $f_p(h)$ are expressed in units of 10^{10} cm and MHz, respectively. Equation (4) is shown by the dash–dotted line in Figure 7. According to Figure 5, a more rapid change in the electron number density gradient with height is required in our model.

The procedure of constructing a modified Newkirk model representing the observed spectrum is described here. To begin, we selected the time moment $t = 13$, found the observed stripe frequencies in Figure 6, and plotted them as the horizontal dotted lines in Figure 7. This time was chosen to construct the model because here four DPR points cover the entire frequency band of the event. Then we considered the height distribution of the magnetic field and the cyclotron harmonics. The magnetic field gradient must be very similar to the electron number density gradient, since at each time no more than 1-3 harmonics are observed. Figure 4 shows that if the gradients differ considerably, then there must be more harmonics. It is important that without additional information on the magnetic field it is impossible to find in advance the number of the harmonics that participate in the event. First we considered the smallest harmonic number $s = 20$, *i.e.* we chose the set of harmonics $s = 20-30$, and created the corresponding model of the magnetic field. Later we

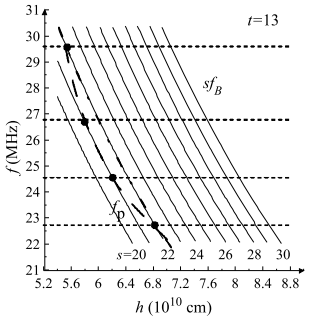

Figure 7 Distributions of the electron plasma frequency (the dash–dotted line for the Newkirk model, the dashed line for the modified Newkirk model used in the proposed model) and the harmonics of the electron cyclotron frequency (solid lines) $s = 20-30$ versus height at time $t = 13$.

discuss alternatives. Thus, in Figure 6 the zebra stripes correspond to the harmonic numbers $s = 20-30$, counted from left to right.

According to Figure 6, at time $t = 13$, the harmonics $s = 21$ and $s = 22$ are present in the spectrum, therefore we chose the magnetic field such that $f_p(h)$ and $22 f_B(h)$ are close to each other. A system of the cyclotron harmonics $s = 20-30$ satisfying these requirements is shown by solid lines in Figure 7. The magnetic field and the cyclotron frequency as functions of height for the chosen set of harmonics $s = 20-30$ can be approximated by

$$B = B_0(t)/(1 + h/7.95)^3, \qquad f_B = f_{B_0}(t)/(1 + h/7.95)^3, \tag{5}$$

where B, f_B, and h are expressed in gauss (G), MHz, and 10^{10} cm, respectively. For $t = 13$ the parameters B_0 and f_{B_0} are the following: $B_0(13) = 2.33$, $f_{B_0}(13) = 6.54$. We note that the specific functional form of the magnetic field on height does not matter much. It is necessary only for the behavior of the function $sf_B(h)$ to be described by the curves close to those shown in Figure 7.

Obviously, the points of intersection of the horizontal dotted lines with the corresponding harmonics $s = 21$ and $s = 22$ denoted by filled circles determine the observed DPR levels, and the dashed line connecting these four DPR points is the electron number density distribution over height providing the observed frequency pattern at $t = 13$. Thus, we have obtained the sought-for modifications to the Newkirk model necessary to explain the observed stripe frequencies at one time.

Following our qualitative scheme, we considered the electron number density to be constant in time during our event, assuming that the frequency drift of the stripes is due to the changing magnetic field. According to Figure 5, the stripes of enhanced radiation as the arcs shown in Figure 6 may be formed due to decrease of the magnetic field in time. To find the magnetic field at times before or after $t = 13$, the magnetic field therefore needs to be increased or decreased, respectively.

The general quantitative picture of the event is given in Figure 8. Here the horizontal dotted lines denote the observed frequencies of the zebra stripes at times $t = 9-12, 14, 17, 19, 22, 28$ (according to Figure 6) shown in the right upper corner of each panel. As in Figure 7, the dashed line describes the obtained variation of the plasma frequency f_p with height, and the solid lines represent the cyclotron frequency harmonics sf_B as a function of height h. The numerals indicate the harmonic numbers. The intersection points of the curves $f_p(h)$ and $sf_B(h)$, *i.e.* DPR points, are denoted by filled circles. If they coincide with the observed ZP frequencies located at the horizontal dotted lines, then the model fits the observations.

At the initial moment $t = 9$, only one DPR point exists (Figures 6 and 8a), and the calculated parameters in Equation (5) are $B_0(9) = 2.62$ and $f_{B_0}(9) = 7.54$. The increase of

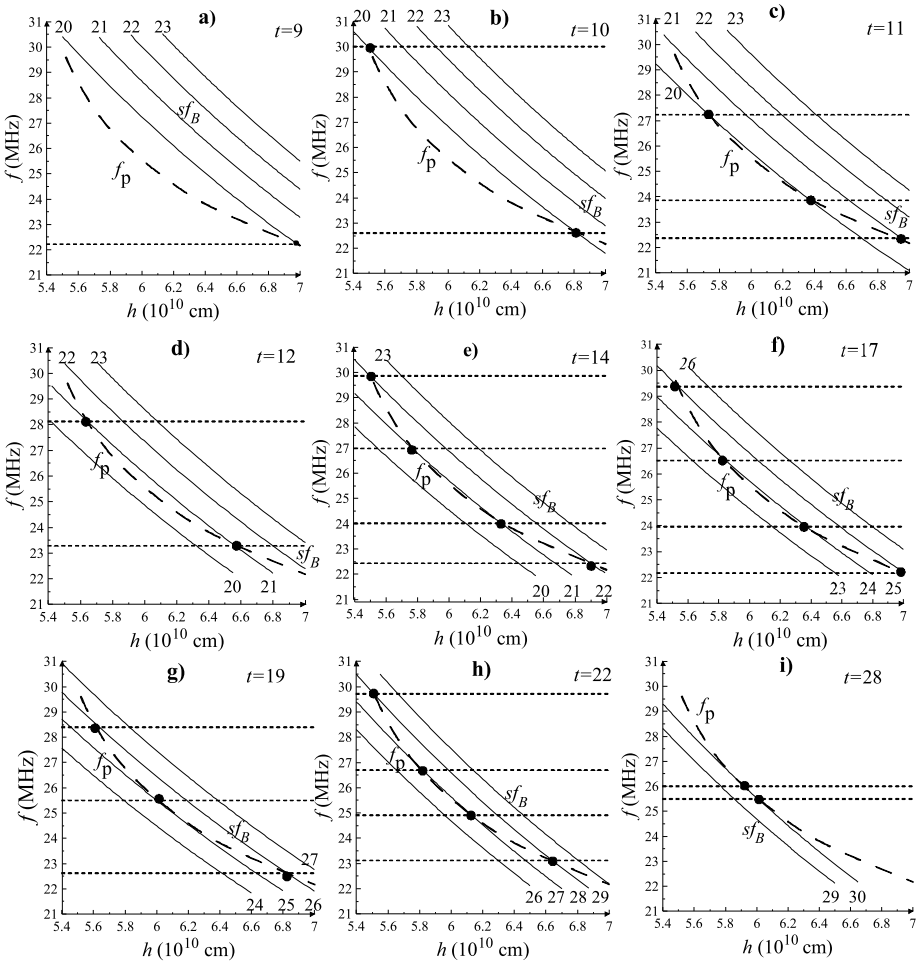

Figure 8 The model of the source based on the assumption that the electron number density is constant in time and the magnetic field decreases in time. The plasma frequency $f_p(h)$ (dashed lines) and the frequencies of the cyclotron harmonics $sf_B(h)$ (solid lines) at different times are plotted against height h. The filled circles at the intersections denote the DPR points.

the magnetic field with respect to $t = 13$ is calculated in such a way that the harmonic $s = 20$ intersects the curve $f_p(h)$ at the frequency $f = 22.2$ MHz, corresponding to the observed ZP frequency.

To shift the frequency of the zebra stripe $s = 20$ from the value $f = 22.2$ MHz in Figure 8a at $t = 9$ to the frequency $f = 22.9$ MHz in Figure 8b at $t = 10$, it is necessary to decrease the magnetic field by 3 %. Surprisingly, the second DPR point automatically coincides with the observed frequency $f = 30$ MHz at the high-frequency wing of the zebra stripe $s = 20$. When the magnetic field decreases by another 3 %, the DPR points at the harmonic $s = 20$ approach each other and shift toward the frequencies that are the observed ZP frequencies at the next moment $t = 11$ (Figure 8c). Moreover, this decrease in the magnetic field causes the intersection point of the harmonic $s = 21$ with the line $f_p(h)$ to arise just at the frequency where the next zebra stripe is observed.

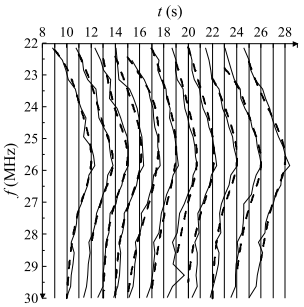

Figure 9 Comparison of the observed spectrum (solid lines) with a calculated smoothed spectrum (dashed lines) in the source model given in Figures 7 – 8.

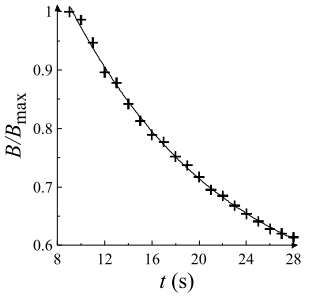

Figure 10 Relative reduction in the magnetic field with time that is necessary to fit the observed spectrum in the source model given in Figures 7 – 8.

It is important that the change in the magnetic field is selected such that one of the DPR points, *i.e.* the intersection point of the lines $f_{\mathrm{p}}(h)$ and $sf_B(h)$, is located on the horizontal line corresponding to the observed ZP frequency at the next moment. Wherein, there is no reason for the rest of the DPR points to coincide with the observed frequencies of the zebra stripes at the 'right' harmonics. Three curves, $f_{\mathrm{p}}(h)$, $sf_B(h)$, and the observed frequency (horizontal line), cannot intersect at the same point by chance. The fact that this coincidence occurs automatically proves that the selected height variations of the magnetic field and electron number density correctly describe the behavior of the parameters in the source.

Furthermore, we successively reduced the magnetic field by approximately 3 % per second, and every time we obtained the coincidence of the model values of the DPR frequencies with the observed ZP frequencies. At the end of the event, the rate of the magnetic field reduction that is necessary to reproduce the observed frequencies, was 1.5 %. For illustration, we give the source models at times $t = 12, 14, 17, 19, 22$, and 28 (Figures 8d – i, respectively). The agreement of the expected and observed stripe frequencies is beyond doubt.

Figure 9 gives the resulting dynamic spectrum for all harmonics in the time interval $t = 9 – 28$. The solid and dotted lines represent the observed and calculated (smoothed) spectra, respectively. Evidently, the suggested source model with decreasing magnetic field explains quite well the observed details of the fingerprint burst in the analyzed time period of the event.

As was mentioned above, to explain the observed frequency drift in the selected portion (Figure 1a) of the fingerprint burst, the magnetic field needs to decrease by approximately 3 % per second at the beginning and by 1.5 % per second at the end of the event. Figure 10 shows the relative change in the magnetic field during the entire period of the event. Evidently, the total change must be rather significant, by approximately 40 % for 18 s. The magnetic field in the source estimated under the assumption that the observed harmon-

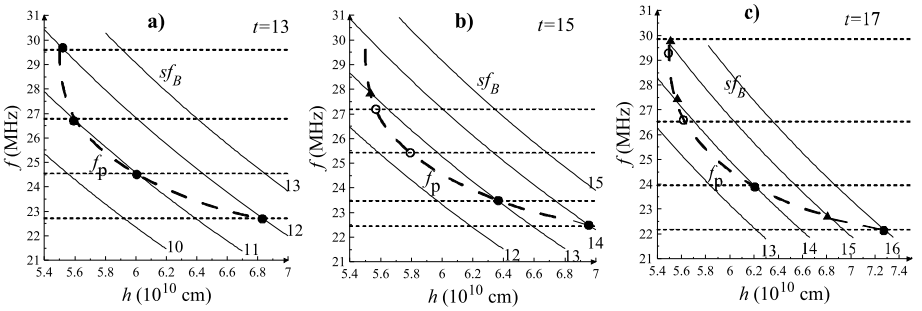

Figure 11 The same as in Figure 8, but for the harmonic numbers $s = 10 - 20$ at three times indicated in the upper right corner of each panel. The filled circles denote the DPR points coinciding with the observed ZP frequencies, open circles denote the intersection points of the line $f_p(h)$ with the observed frequencies that are not DPR points, and triangles denote the DPR points not coinciding with the observed ZP frequencies.

ics correspond to $s = 20-30$ is found to be $B \approx 0.3-0.5$ G, which is quite usual for the decameter burst sources emerging from heights on the order of several hundred thousand kilometers above the photosphere.

4.3. Alternative Models of the Fingerprint Burst

First of all, we discuss the harmonic numbers assigned in the source model for the quantitative explanation of the fingerprint spectrum. Calculations show that using the smaller harmonic numbers to interpret the data selected in Figure 1 is unsuccessful. This follows from Figure 11, where the attempt to fit the observations using harmonics $s = 10-20$ is shown.

Similar to the set of harmonics $s = 20-30$, we selected similar height gradients of the plasma frequency and the tenth harmonic of the cyclotron frequency. Then, using the four observed ZP frequencies at the moment $t = 13$, we plotted the possible modification to the plasma frequency expected from the Newkirk model (Figure 11a). To achieve coincidence of the DPR points with the observed frequencies in the subsequent times, the magnetic field must decrease more quickly than in this model (by 6 – 7 % per second). What is more important, no coincidence over all the four points was obtained in the subsequent times by decreasing the magnetic field.

Figures 11b – c show the magnetic field distributions versus height at the times $t = 15$ and $t = 17$ obtained for the magnetic field reduction that gives the best fit for the observed ZP frequencies at the times given in Figure 6 (the harmonic numbers were changed from $s = 20-30$ to $s = 10-20$). Filled circles denote the DPR points (the points where the model value of the plasma frequency is equal to the frequency of the cyclotron harmonic) coinciding with the observed ZP frequencies, which are located on the horizontal dotted lines. Open circles refer to the frequencies of the observed zebra stripes on the line $f_p(h)$, *i.e.* the points through which the corresponding harmonics 'must' pass. In Figure 11b ($t = 15$) the magnetic field is reduced by 13 % compared to $t = 13$, and two DPR points in the low-frequency wing of the spectrum coincide with the observed ZP frequencies. However, in the high-frequency part the model and observed curves move away from each other. According to observations, the curve corresponding to the harmonic $s = 12$ must touch the curve $f_p(h)$ at 25.5 MHz at a point shown by the open circle, but at this frequency, the two mentioned curves are well separated. In addition, the very high frequency DPR point denoted by a

triangle is not located at the observed frequency 27.2 MHz. Figure 11c relating to $t = 17$ demonstrates still greater divergence of the observed ZP frequencies and the values required by the model. Here, the magnetic field is decreased by 9 % compared to $t = 15$ to provide the intersection of the curve corresponding to the harmonic $s = 14$ with the curve $f_p(h)$ at the horizontal line denoting the observed frequency 24.0 MHz. But the remaining three DPR points are not located at the horizontal lines, that is, they differ markedly from the observed ones. At later times the coincidence is no longer obtained because the harmonics with relatively low numbers are too widely separated.

A similar attempt to create the model with the harmonic numbers $s = 30 - 40$ also failed. In this case, the harmonics were located too close to the neighboring ones, and the coincidence of the observed and calculated values could not be reached. In addition, we note that the high numbers of harmonics can result in a breaking of the conditions of electron trapping in a magnetic trap since the plasma parameter

$$\beta = 8\pi\kappa T N/B^2 = 2\left(f_p^2/f_B^2\right)\left(v_T^2/c^2\right), \tag{6}$$

describing the ratio between the gas pressure and magnetic pressure, is no longer negligibly small.

It is worth noting, however, that to fit the spectrum by harmonics of $s = 20 - 30$ does not guarantee an accurate measurement of the magnetic field in the ZP source. First, it is clear that the model can be adapted to other sets of harmonics, for example, $s = 18 - 28$ or $s = 23 - 33$. Second, this model assumed a simple decreasing magnetic field that is the same at all heights. At the same time, the magnetic field distribution over the source can change in a more complicated way, for example, by variation of the gradient. However, the example given above for the harmonic set $s = 10 - 20$ shows that the model does not permit an arbitrary choice of the harmonic numbers.

As mentioned above, the harmonic numbers $s = 20 - 30$ were only derived for the portion of the dynamic spectrum in the time interval 08:32:09 UT – 08:32:28 UT in Figure 1. Before this time period, one can also distinguish quasi-vertical arcs as zebra stripes. A similar analysis shows that the spectrum before 08:32:09 UT contained the harmonics with numbers down to $s = 5$. This fact also favors the correctness of the derived harmonic numbers.

The properties of the fingerprint spectrum can also be explained by a source model with somewhat different height distributions of the magnetic field and electron number density. An example of such distributions is given in Figure 12. In this model, the electron number density is exactly the Newkirk distribution, and the magnetic field is a convex function of height, unlike Equation (5). It is easy to see that the model leads to the dynamic spectrum with a set of quasi-vertical arcs with the opposite directions of the frequency drift in the high- and low-frequency wings. Figures 12a – c show that the intersection of the curve $f_p(h)$ with increasingly higher harmonics $sf_B(h)$ results in the DPR points that are closer to each other and later disappear from the resonance. Thus, the main properties of the fingerprint spectrum can be qualitatively explained in such a model.

Following the technique described previously, one can find the rate of the magnetic field decrease that reproduces the model DPR points agreeing with the observed ZP frequencies at subsequent times. However, the analysis shows that if the magnetic field is simply reduced without changing its functional form, it is impossible to reproduce the observations. Figures 12b – c show that the magnetic field distribution that reproduces observations at $t = 13$ leads to a significant difference between the calculated DPR points and the observed ZP frequencies at subsequent times (DPR points denoted by triangles are far away from the measured ZP frequencies denoted by open circles).

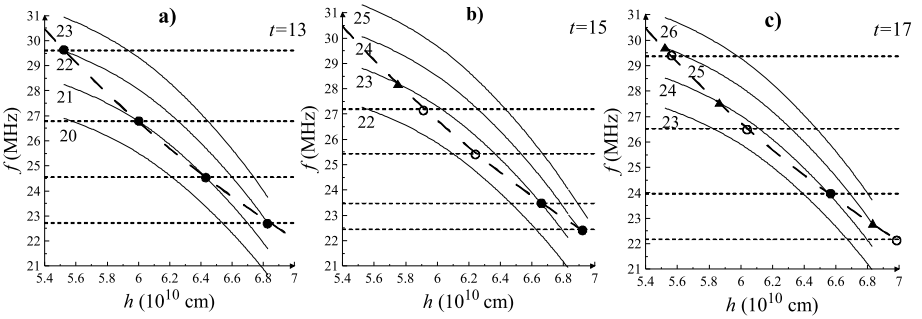

Figure 12 The source model based on the assumption that the electron number density follows Newkirk's model (constant in time) and the magnetic field is a convex function of h and decreases in time. Plasma frequency $f_p(h)$ (dashed line) and the frequencies of the cyclotron harmonics $sf_B(h)$ (solid lines) are plotted against height h at three times. The symbols used are the same as in Figure 11.

Figure 13 The source model based on the assumption that the electron number density distribution moves up in the corona, and the magnetic field is constant in time. The electron plasma frequency $f_p(h)$ (dashed line) and the frequencies of the cyclotron harmonics $sf_B(h)$ (solid lines) are plotted against height h at three times. The symbols used are the same as in Figure 11.

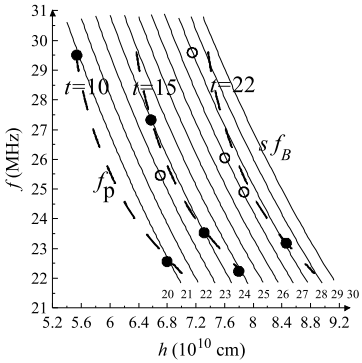

Next we considered that the electron number density distribution takes the form of the modified Newkirk model, but its magnitude is changed so that the plasma frequency increases in time (the dashed line in Figure 7 moves upward), and the magnetic field remains constant. Evidently, the main property of the fingerprint spectrum, namely, the presence of two DPR points at a given harmonic, their approach with time and disappearance, is quite explainable under this assumption. However, the increasing electron number density eventually causes the DPR points to deviate from the observed frequency band.

As another option, we assumed that the electron number density distribution moves upward in the corona, that is, moves to the right in Figure 13. Again a good coincidence of the calculated and observed frequencies cannot be achieved, although Figure 13 indicates that the discrepancy is not so significant as for the other models. Furthermore, the assumed motion of the electron number density distribution in the background corona must be accompanied by simultaneous motion of the region of the non-equilibrium electrons, which is hard to realize. In this model, the source must travel the distance of 1.7×10^{10} cm in 12 s, which implies a high velocity of 1.5×10^9 cm s^{-1}. This exceeds the sound velocity at an appropriate temperature ($v_s \approx 10^7$ cm s^{-1}) by two orders of magnitude.

Therefore, all the considered variants appear less able to form the fingerprint spectrum than the model with changing magnetic field shown in Figure 8.

5. Discussion and Conclusions

The fine structure of the solar decameter radiation as a fingerprint spectrum was explained in the framework of the DPR mechanism working in the magnetic trap. The successful model adopted a specific height distribution of the electron number density that is a slight modification of the Newkirk (1961) model and a relatively fast change in the magnetic field with time. The main properties of the fingerprint spectrum, namely, the fast frequency drift of the zebra stripes, the presence of two frequencies of peak brightness in a given harmonic at a given time, and the opposite direction of the frequency drift at these frequencies, automatically follow from the model. The proposed model was realized with reasonable parameters for the trap. The source is located at the height $h \approx (5-7) \times 10^{10}$ cm above the photosphere, the electron number density varies within $N \approx (0.6-1.1) \times 10^7$ cm^{-3}, and the magnetic field is $B \approx 0.3-0.5$ G.

The estimations given above only refer to the time period shown by a rectangle in Figure 1. If the whole burst fingerprint is considered, then judging from the low-frequency boundary of the spectrum ($f = 15$ MHz), we can estimate that the source extends up to the heights of about $h \approx 10^{11}$ cm, and the low boundary of the electron number density is $\approx 3 \times 10^6$ cm^{-3}.

It should be noted that the change in the magnetic field occurs simultaneously over the entire height of the source, that is, in the interval $h \approx (5-10) \times 10^{10}$ cm corresponding to the observed frequency band $f \approx 20-30$ MHz. The source may extend to lower heights (higher frequencies) because the low-frequency boundary is clearly seen in the spectrum, while the high frequency boundary may be cut off by the boundary of the available frequency band of observations.

Simultaneous change in the magnetic field over the entire height of the source implies that the observed zebra stripes as quasi-vertical arcs cannot be associated with any perturbation propagating along the loop in the corona, but are due, most probably, to some process involving the whole loop. The best candidate for such a process are nonlinear fast magneto-acoustic (FMA) oscillations of the magnetic flux tube, which are accompanied by compression and depression of the magnetic field. This idea is developed in the following arguments.

As we showed in Figure 1b, the fingerprint burst discussed above was not a single event; there are at least three identical bursts that form a quasi-periodical sequence with a period of about 60 s. The closeness of the spectral parameters of three bright elements in Figure 1b (frequency band, stripe spacing, and frequency drift rate) implies that they originated from the same source and were generated by the same process. According to our model, these elements are associated with the decreasing magnetic field, and the magnitudes of the magnetic field should be approximately the same. Obviously, to start the decrease from the same values as in the previous element, the magnetic field needs to resume its initial magnitude. In the dynamic spectrum such a process could result in the 'ascending' arcs with opposite curvature between the observed 'descending' arcs. But the spectrum under consideration only shows 'descending' arcs: when the magnetic field increases, the DPR instability weakens or disappears, and when the magnetic field decreases, it is revived again. This effect can be understood under the assumption that it is due to the fast magneto-acoustic (FMA) oscillations of the magnetic flux tube.

FMA oscillations result in the periodic compression and depression of the magnetic field in the magnetic flux tube containing the source of the fingerprint source as a magnetic trap. When the tube is compressed, the mirror ratio decreases in the source, which results in the partial particle precipitation from the trap. In steps of the tube depression, the magnetic

field in the source decreases, the local mirror ratio increases, and the fast electron number density increases again, leading to a revival of the generation process. We note that the weak 'ascending' arcs can be distinguished in Figure 1b at times before the appearance of the bright 'descending' stripes (at 08:30:28, 08:31:40, 08:32:30 UT). This is also consistent with the assumption that FMA oscillations are the reason for the magnetic field change in the fingerprint source.

Numerical estimations also confirm this idea. The period of the FMA oscillations is determined by the relation (Stepanov, Zaitsev, and Nakariakov, 2012)

$$T \approx \frac{2.5r}{V_{\mathrm{A}}}, \tag{7}$$

where r is the radius of the magnetic flux tube cross-section and V_{A} is the Alfvén velocity

$$V_{\mathrm{A}} = \frac{B}{\sqrt{4\pi m_{\mathrm{i}} N}} = c\frac{f_B}{f_{\mathrm{p}}}\sqrt{\frac{m}{m_{\mathrm{i}}}} \tag{8}$$

(m_{i} is the ion mass). Since the Alfvén velocity only depends on the ratio f_B/f_{p}, in the DPR regions where $f_B/f_{\mathrm{p}} = 1/s$, it remains constant and only depends on the harmonic number s:

$$V_{\mathrm{A}} = \frac{c}{s}\sqrt{\frac{m}{m_{\mathrm{i}}}}. \tag{9}$$

For the selected set of harmonics $s = 20-30$, the Alfvén velocity takes quite reasonable values $v_{\mathrm{A}} \approx (2.3-3.5)10^7$ cm s^{-1}. The oscillation period

$$T \approx \frac{2.5r}{c}\, s\sqrt{\frac{m_{\mathrm{i}}}{m}} \tag{10}$$

for $s = 20-30$ is consistent with the observed value $T \approx 60$ s if the tube radius is $r \approx (5-8) \times 10^8$ cm, which does not contradict the known data about the coronal magnetic loop cross-section. The nonlinear character of the oscillations easily permits a significant change in the magnetic field strength in time, which is necessary to explain the fingerprint spectrum within the framework of the proposed interpretation.

It should be noted that the FMA oscillations contain not only a change in the magnetic field, but also a change in the electron number density. However, the relative change in the electron number density can be neglected for low values of the parameter β given by Equation (6) (Pikel'ner, 1964).

Thus, the presented model of the source is able to explain the details of the unusual frequency drift of the stripes of enhanced intensity in the observed fingerprint spectrum within the framework of the DPR mechanism under quite reasonable physical conditions in the coronal magnetic trap. The necessary properties of the source model are, first, the closeness of the gradients of the magnetic field and the electron number density (to provide few zebra stripes at a given moment), and second, the opposite signs of these gradients at the upper and lower parts of the source (to provide different signs of the frequency drift in the high- and low-frequency parts of the spectrum). Of course, the selected harmonic numbers, the proposed form of the electron number density distribution, and the height variations in the magnetic field cannot be found unambiguously from the observed spectral features. However, as we showed above, the proposed model provides a quite good quantitative match of the observed and predicted model parameters of the fingerprint burst, and it gives reliable estimates of the physical conditions in the burst source.

References

Aurass, H., Klein, K.-L., Zlotnik, E.Ya., Zaitsev, V.V.: 2003, *Astron. Astrophys.* **410**, 1001.

Braude, S.Y., Megn, A.V., Ryabov, B.P., Sharykin, N.K., Zhouck, I.N.: 1978, *Astron. Astrophys. Suppl.* **54**, 3.

Chen, B., Bastian, T.S., Gary, D.E., Jing, J.: 2011, *Astrophys. J.* **736**, 64.

Chernov, G.P.: 2006, *Space Sci. Rev.* **127**, 195.

Kuijpers, J.: 1975, *Astron. Astrophys.* **40**, 405.

Kuznetsov, A.A., Tsap, Yu.T.: 2007, *Solar Phys.* **241**, 127.

Melnik, V.N., Konovalenko, A.A., Abranin, E.P., Dorovskyy, V.V., Stanislavsky, A.A., Rucker, H.O., Lecacheux, A.: 2005, *Astron. Astrophys. Trans.* **24**, 391.

Melnik, V.N., Rucker, H.O., Konovalenko, A.A., Dorovskyy, V.V., Abranin, E.P., Brazhenko, A.I., Thide, B., Stanislavskyy, A.A.: 2008, In: Wang, P. (ed.) *Solar Physics Research Trends*, Nova Science Publishers, New York, 287.

Melnik, V.N., Rucker, H.O., Konovalenko, A.A., Dorovskyy, V.V., Abranin, E.P., Lecacheux, A.: 2011, In: Rucker, H.O., Kurth, W.S., Louarn, P., Fischer, G. (eds.) *Planetary Radio Emissions VII*, Austrian Academy of Sciences Press, Vienna, 343.

Newkirk, G.: 1961, *Astrophys. J.* **131**, 983.

Pikel'ner, S.B.: 1964, *Fundamentals of Cosmic Electrodynamics*. *NASA Tech. Trans.* **F-175**, 93.

Stepanov, A.V., Zaitsev, V.V., Nakariakov, V.M.: 2012, *Coronal Seismology*, Wiley/VCH, Berlin, 45.

Winglee, R.M., Dulk, G.: 1986, *Astrophys. J.* **307**, 808.

Zheleznyakov, V.V.: 2000, *Radiation in Astrophysical Plasmas*, Kluwer Academic, Dordrecht, 389.

Zheleznyakov, V.V., Zlotnik, E.Ya.: 1975a, *Solar Phys.* **43**, 431.

Zheleznyakov, V.V., Zlotnik, E.Ya.: 1975b, *Solar Phys.* **44**, 461.

Zlotnik, E.Ya.: 2009, *Cent. Eur. Astrophys. Bull.* **33**, 281.

Zlotnik, E.Ya., Sher, E.M.: 2009, *Radiophys. Quantum Electron.* **52**, 88.

Zlotnik, E.Ya., Zaitsev, V.V., Altyntsev, A.T.: 2014, *Solar Phys.* **289**, 233.

Zlotnik, E.Ya., Zaitsev, V.V., Aurass, H., Mann, G., Hofmann, A.: 2003, *Astron. Astrophys.* **410**, 1011.